Supporting Information for "A Case Study on Drivers of the Isotopic Composition of Water Vapour at the Coast of East Antarctica"

Riqo Chaar[1,*], Armin Sigmund[1,*], Pirmin Philipp Ebner[2], Michael Lehning[1,3]

[1]CRYOS, School of Architecture, Civil and Environmental Engineering, EPFL, Lausanne, Switzerland

[2]Geophysical Institute and Bjerknes Centre for Climate Research, University of Bergen, Bergen, Norway

[3]WSL Institute for Snow and Avalanche Research SLF, Davos, Switzerland

*These authors contributed equally to this work

Contents of This File

1. Text S1 to S4

2. Figures S1 to S4

3. Table S1

Introduction

Texts S1 to S3 describe methodological details of the model parts used to (i) compute the isotopic composition of the surface snow and sublimation flux across Antarctica (*Model Sublimation*) and (ii) the isotopic composition of air parcels exchanging moisture with snow and ocean surfaces and experiencing cloud formation (*Model Air Parcel*). In Text S4, we compare the estimates of the isotopic compositions of surface snow and atmospheric vapour in *Model Sublimation* with measurements from Dome C, East Antarctica.

Text S1. Basic Equations for Stable Water Isotopes

The isotopic composition (δ_{i}) throughout this manuscript is formulated in delta notation and given in ‰ (Craig, 1961):

$$\delta_{\mathrm{i}} = \frac{R_{\mathrm{i}}}{R_{\mathrm{i,VSMOW}}} - 1 \ . \tag{1}$$

Here, the subscript i refers to a heavy water isotopologue ($H_2{}^{18}O$ or $HD^{16}O$), R_{i} is the abundance ratio of heavy to light water isotopologues and $R_{\mathrm{i,VSMOW}}$ is the reference isotopic ratio of the Vienna Standard Mean Ocean Water (VSMOW) listed in Table S1 together with other constants and parameters.

The isotopic ratio can be expressed as

$$R_{\mathrm{i}} = \frac{m_{\mathrm{i}}}{m_{\mathrm{H_2{}^{16}O}}} \ \frac{M_{\mathrm{H_2{}^{16}O}}}{M_{\mathrm{i}}} \ , \tag{2}$$

where $m_{\mathrm{H_2{}^{16}O}}$ is the mass of the light isotopologue in a water sample, m_{i} is the mass of a heavy isotopologue ($H_2{}^{18}O$ or $HD^{16}O$), and $M_{\mathrm{H_2{}^{16}O}}$ and M_{i} are the respective molecular masses.

For given values of $R_{\mathrm{H_2{}^{18}O}}$, $R_{\mathrm{HD^{16}O}}$, and the total mass of a water sample ($m_{\mathrm{tot}} = m_{\mathrm{H_2{}^{16}O}} + m_{\mathrm{H_2{}^{18}O}} + m_{\mathrm{HD^{16}O}}$), the masses of the individual isotopologues are known, e.g.:

$$m_{\mathrm{H_2{}^{18}O}} = m_{\mathrm{tot}} \left(1 + \frac{M_{\mathrm{H_2{}^{16}O}} + R_{\mathrm{HD^{16}O}} \ M_{\mathrm{HD^{16}O}}}{R_{\mathrm{H_2{}^{18}O}} \ M_{\mathrm{H_2{}^{18}O}}} \right)^{-1} \ . \tag{3}$$

The equilibrium fractionation factor ($\alpha_{\mathrm{X-V}}$) is defined as

$$\alpha_{\mathrm{X-V}} = \frac{R_{\mathrm{X}}}{R_{\mathrm{V}}} > 1 \ , \tag{4}$$

where the subscript X refers to the solid (S) or liquid (L) phase and the subscript V refers to the vapour phase. These factors are computed as a function of surface temperature, which is taken from the ERA5 reanalysis data. The $\alpha_{\mathrm{S-V}}$ factors for $H_2{}^{18}O$ and $HD^{16}O$

are calculated according to Majoube (1970) and Merlivat and Nief (1967), respectively. For $\alpha_{\mathrm{L-V}}$, the formulas of Majoube (1971) are used.

Text S2. Details of *Model Sublimation*

The isotopic composition of the sublimation flux is computed from that of the surface snow assuming equilibrium fractionation (Equation 4). To simulate changes in the isotopic composition of surface snow with time, *Model Sublimation* parameterizes the mass of each water isotopologue in snowfall and in the surface vapour flux. The model neglects liquid precipitation on the ice sheet, i.e., rain-on-snow events, which are rare in Antarctica. To represent the case of vapour deposition, *Model Sublimation* estimates the isotopic ratio of the atmospheric vapour ($R_{\mathrm{i,V}}$) as

$$R_{\mathrm{i,V}} = 0.5 \left(\frac{R_{\mathrm{i,snow}}}{\alpha_{\mathrm{S-V}}(T)} + \frac{R_{\mathrm{i,p}}}{\alpha_{\mathrm{S-V}}(\overline{T}_{\mathrm{a}})} \right) , \tag{5}$$

where T is surface temperature, $\overline{T}_{\mathrm{a}}$ (K) is the daily running mean air temperature at a height of 2 m, and $R_{\mathrm{i,snow}}$ and $R_{\mathrm{i,p}}$ are the isotopic ratios of surface snow and potential snowfall, respectively. Assuming equilibrium fractionation and multiplying Equation 5 with $\alpha_{\mathrm{S-V}}(T)$ yields the isotopic ratio of the deposition flux ($R_{\mathrm{i,flx}}$):

$$R_{\mathrm{i,flx}} = 0.5 \left(R_{\mathrm{i,snow}} + \frac{\alpha_{\mathrm{S-V}}(T)}{\alpha_{\mathrm{S-V}}(\overline{T}_{\mathrm{a}})} R_{\mathrm{i,p}} \right) . \tag{6}$$

In the baseline simulation, the isotopic composition of snowfall is parameterized using the empirical function of Stenni et al. (2016), henceforth referred to as Stenni16:

$$\delta^{18}\mathrm{O} = 0.45 \left(\overline{T}_{\mathrm{a}} - 273.15 \right) - 31.21 . \tag{7}$$

This function represents a linear fit to local measurement data from Dome C, averaged over daily intervals, where the air temperatures span the broad range from -80 °C to -20 °C. Although Masson-Delmotte et al. (2008) derived δ_{i}-temperature relationships from a data

set with many Antarctic sites, these relationships are not suitable for our purpose because they are based on yearly averages and a variety of snow samples including ice cores, firn cores, snow pits, and precipitation. In a sensitivity study, we perform simulations with other local δ^{18}O-temperature relationships for snowfall, namely those for Vostok from Landais, Ekaykin, Barkan, Winkler, and Luz (2012), henceforth Landais12,

$$\delta^{18}\mathrm{O} = 0.35 \left(\overline{T}_\mathrm{a} - 273.15\right) - 40 \ , \tag{8}$$

and for Dome Fuji from Fujita and Abe (2006), henceforth FA06,

$$\delta^{18}\mathrm{O} = 0.78 \left(\overline{T}_\mathrm{a} - 273.15\right) - 18.4 \ . \tag{9}$$

Equations 8 and 9 are based on data in the temperature range from -76 °C to -44 °C and from -76 °C to -28 °C, respectively. For all of these options, δD of the snowfall is derived using the $\delta^{18}\mathrm{O} - \delta\mathrm{D}$ relationship from Masson-Delmotte et al. (2008),

$$\delta\mathrm{D} = (7.75 \ \delta^{18}\mathrm{O}) - 4.93 \ . \tag{10}$$

We initialise Model Flux by assuming that a large quantity of snowfall has just occurred. Hence, for a particular location, the initial isotopic composition of all snow layers is the same. In the surface snow layer, the mass balance for each water isotopologue is

$$m_\mathrm{i}|_t^1 = m_\mathrm{i}|_{t-1}^1 + m_{\mathrm{i,p}}|_t + m_{\mathrm{i,flx}}|_t \begin{cases} -f \ m_\mathrm{i}|_{t-1}^1 & \text{if } \Delta m|_t \geq 0 \ , \\ +f \ m_\mathrm{i}|_{t-1}^2 & \text{if } \Delta m|_t < 0 \ , \end{cases} \tag{11}$$

where, $m_\mathrm{i}|_t^1$ and $m_\mathrm{i}|_{t-1}^1$ are the masses of a specific water isotopologue (i) in the surface snow layer at time step t and the previous time step $(t-1)$, respectively; $m_{\mathrm{i,p}}|_t$ is the mass added by precipitation; $m_{\mathrm{i,flx}}|_t$ is the mass added or removed (positive or negative sign, respectively) by the surface flux; $m_\mathrm{i}|_{t-1}^2$ is the mass of the water isotopologue in the layer below the surface snow layer; and f is the absolute ratio between the net mass gain

or loss at the surface ($\Delta m|_t$) and the total mass of the snow layer. For layers below the surface snow layer ($n > 1$), the balance equation becomes

$$m_{\mathrm{i}}|_t^n = m_{\mathrm{i}}|_{t-1}^n - f\, m_{\mathrm{i}}|_{t-1}^n + \begin{cases} f\, m_{\mathrm{i}}|_{t-1}^{n-1} & \text{if } \Delta m|_t \geq 0\ , \\ f\, m_{\mathrm{i}}|_{t-1}^{n+1} & \text{if } \Delta m|_t < 0\ , \end{cases} \tag{12}$$

where n is the number of the layer. For the lowest layer ($n = 100$), the term $m_{\mathrm{i}}|_{t-1}^{n+1}$ is not known and assumed to be equal to $m_{\mathrm{i}}|_{t-1}^{n}$.

Text S3. Details of *Model Air Parcel*

For each air parcel, we consider time intervals of 3 h centered around data points from the trajectory data set. Due to these centered intervals, the first and the last interval are only 1.5 h long. For each interval, we use ERA5 reanalysis data for the closest grid cell and the hour beginning at the center of the air parcel interval. The only exception is the last interval, for which we use ERA5 data in the hour ending at the center of the interval, i.e., in the last hour before the parcel arrives at the ship.

During ocean evaporation, equilibrium and kinetic fractionation are modelled using the Craig-Gordon formula (e.g. Horita et al., 2008),

$$\delta_{\mathrm{E}} = \frac{\alpha_{\mathrm{L-V}}^{-1}\ \delta_{\mathrm{L}} - h_{\mathrm{s}}\ \delta_{\mathrm{A}} - (\varepsilon * + \varepsilon_{\mathrm{k}})}{1 - h_{\mathrm{s}} + 10^{-3}\ \varepsilon_{\mathrm{k}}}\ , \tag{13}$$

where the isotopic composition of ocean water (δ_{L}) is set to $\delta^{18}\mathrm{O} = -0.5‰$ or $\delta\mathrm{D} = -1.7‰$, which is typical for surface water in the Southern Ocean (LeGrande & Schmidt, 2006; Bonne et al., 2019); δ_{E} and δ_{A} are the isotopic compositions of the evaporation flux and the air parcel, respectively; h_{s} is the ratio of ambient vapour pressure (here evaluated at a height of 2 m) and saturation vapour pressure at the surface; and $\varepsilon* = (1 - \alpha_{\mathrm{L-V}}^{-1})10^3 > 0$ and $\varepsilon_{\mathrm{k}} = (1 - \alpha_{\mathrm{k}}^{-1})10^3 > 0$ are functions of the equilibrium ($\alpha_{\mathrm{L-V}}$) and

kinetic (α_{k}) fractionation factors, respectively. The expression for ε_{k} is parameterized as

$$\varepsilon_{\mathrm{k}} = (1 - h_{\mathrm{s}})\ \theta \left[1 - \left(\frac{D_{\mathrm{i}}}{D}\right)^{n}\right] 10^{3}\ , \tag{14}$$

where the ratio of diffusion coefficients for the heavy and light water isotopologues (D_{i}/D) is taken from Merlivat (1978). For the exponent, a value of $n = 0.5$ is assumed, which is typical for open water bodies in natural conditions (Gat et al., 2001). The term θ is approximated with a value of $\theta = 1$, which is appropriate if h_{s} and δ_{A} are evaluated in the lower part of the boundary layer, where they are directly influenced by evaporation (Gat et al., 1996). If h_{s} approaches a value of 1, Equation 13 will yield a δ_{E} value approaching $\pm$ infinity depending on δ_{A}. At the same time, propagated errors in δ_{E} will approach infinity (Kumar & Nachiappan, 1999). To avoid implausible isotopic compositions, δ_{E} is limited to minimum and maximum values of $-1000‰$ and $+10000‰$, respectively, corresponding to isotopic ratios of zero and approximately 11 times the VSMOW values, respectively.

To initialize air parcels over the ocean, Equation 13 is simplified using the global closure assumption. Taking into account Equation 1, this simplification yields (e.g. Dar et al., 2020)

$$R_{\mathrm{E}} = \frac{\alpha_{\mathrm{k}} R_{\mathrm{L}}}{\alpha_{\mathrm{L-V}}(1 - h_{\mathrm{s}} + \alpha_{\mathrm{k}} h_{\mathrm{s}})}\ , \tag{15}$$

where R_{E} and R_{L} are the isotopic ratios of the evaporation flux and the ocean, respectively. Air parcels which are initialized over snow, begin their journey with isotopic ratios according to Equation 5.

While the volume of the air parcel (V) stays constant, its mass (m_{A}) changes according to the ideal gas law,

$$m_{\mathrm{A}} = \frac{p\ V}{R_{\mathrm{d}}\ T_{\mathrm{v}}}\ , \tag{16}$$

where p is air pressure, R_{d} is the specific gas constant of dry air, and T_{v} is virtual temperature. If the specific humidity of the parcel exceeds its saturation value, the model will account for cloud formation and preciptation by reducing the vapour mass to reach the saturation specific humidity. The effect of this phase change and mass removal on the isotopic composition of the parcel is computed using the classic Rayleigh distillation model in its integrated form (Sinclair et al., 2011),

$$\delta_{\mathrm{i},2} = (1000 + \delta_{\mathrm{i},1}) \left(\frac{q_2}{q_1} \right)^{\hat{\alpha}_{\mathrm{X-V}}-1} - 1000 \ , \tag{17}$$

where $\delta_{\mathrm{i},1}$ and q_1 are, respectively, the isotopic composition and specific humidity of the parcel after accounting for surface exchange and before accounting for cloud formation, $\delta_{\mathrm{i},2}$ and q_2 are, respectively, the isotopic composition and specific humidity of the parcel after accounting for cloud formation, and $\hat{\alpha}_{\mathrm{X-V}}$ is a weighted average of the equilibrium fraction factors for the liquid-vapour and solid-vapour transitions, considering a cloud ice fraction that increases linearly from 0 to 1 in the temperature range from 0°C to −20°C.

Text S4. Model-Measurement Comparison for the Location of Dome C

In this section, we analyze the sensitivity of *Model Sublimation* with respect to the settings for snow layer thickness (SLT) and snowfall isotopic composition. In addition to these settings, the fractionation assumption for snow sublimation is varied, i.e., we either assume equilibrium fractionation (Run E) or neglect fractionation (Run N) during sublimation. The model is run for the location of Dome C, in the period from January 2013 to January 2016 and the results are compared with isotope measurements for surface snow and atmospheric water vapour, published by Casado et al. (2016, 2018).

With increasing values of SLT, the modelled isotopic composition of surface snow responds more slowly to the surface flux and snowfall (Figure S1). Using a value of SLT = 1

cm, both Run E and N reproduce well the measured seasonal cycle in surface snow δ^{18}O. For a lower value of SLT = 0.1 cm, the seasonal amplitude is overestimated and the seasonal maxima and minima are attained slightly too early. A value of SLT = 10 cm is clearly too high as the modelled seasonal cycle almost vanishes in this case. Additionally, field observations by Hughes et al. (2021) demonstrate that δ^{18}O can vary significantly between snow layers of 0–0.5 cm, 0–1 cm, 1–2 cm, and 2–4 cm below the snow surface. These conditions can only be represented in the model if the vertical resolution of snow layers is at least in the order of 1 cm. For SLT = 1 cm, the root-mean-square error (RMSE) with respect to the measurements is approximately half of that for SLT = 0.1 cm and therefore, we use a value of SLT = 1 cm in the remaining analysis.

On short time scales, the measured δ^{18}O of surface snow varies more strongly than the simulated one, partly because the sampling location changes slightly with time and the small-scale spatial variability is not represented in the simulations (Casado et al., 2018). Differences between Run E and Run N are visible in austral summer when sublimation plays a signigicant role. These summertime differences become less pronounced with increasing SLT. For SLT = 1 cm, the surface snow δ^{18}O in summer is up to 1.5‰ more enriched in Run E than in Run N.

So far, we have used the snowfall δ-temperature relationship of Stenni16 because it was derived from measurements at Dome C. Figure S2a shows how the surface snow δ^{18}O at Dome C changes when applying snowfall δ-temperature relationships from other Antarctic sites (Equations 8 and 9). This sensitivity test allows us to estimate uncertainties arising from the generalization of a site-specific snowfall δ-temperature relationship. As expected, the relationship of FA06 with a high δ^{18}O-temperature slope leads to an in-

creased seasonal amplitude in the surface snow δ^{18}O. In austral summer, the agreement with the measurements is still reasonable while in austral winter, the surface snow δ^{18}O is clearly too depleted. Overall, the RMSE of the surface snow δ^{18}O is approximately 4‰ for the relationship of FA06, which is 1.7 times higher than for the relationship of Stenni16. Using the relationship of Landais12, the modelled δ^{18}O of the surface snow is systematically too depleted while the seasonal amplitude is only slightly reduced compared to the relationship of Stenni16. The systematic difference is due to a low intercept value in the δ-temperature relationship of Landais12, leading to the highest RMSE of approximately 5‰.

Figure S2b compares the estimated isotopic composition of atmospheric water vapour with measurements at Dome C available in a 24-d period in December 2014 and January 2015. It is important to note that this figure is only based on the simple parameterization used in *Model Sublimation* without considering air parcel trajectories. The comparison with the measurements allows us to assess potential uncertainties in this parameterization, affecting the isotopic composition of the deposition flux in *Model Sublimation* and the initialization of the air parcel δ^{18}O over snow in *Model Air Parcel*.

With the snowfall δ-temperature relationships of Stenni16 and FA06, the estimated vapour δ^{18}O values are very similar and close to the measured mean value for the whole period. In Run E, the vapour δ^{18}O based on the relationship of Stenni16 is characterized by a mean bias error (MBE) of -0.2‰. For the same model run, the RMSE is 3.7‰ because our simple estimate of the vapour δ^{18}O strongly underestimates the measured diurnal variations. The snowfall δ-temperature relationship of Landais12 generally results in too depleted vapour δ^{18}O values at Dome C with a MBE of -4.9‰ and a RMSE of 6.2‰ for

Run E. These findings suggests that the initial air parcel $\delta^{18}O$ over snow may be under- or overestimated by a few ‰ depending on where and when the air parcel is initialized.

References

Bonne, J.-L., Behrens, M., Meyer, H., Kipfstuhl, S., Rabe, B., Schönicke, L., ... Werner, M. (2019). Resolving the controls of water vapour isotopes in the Atlantic sector. *Nature Communications*, *10*(1), 1632.

Casado, M., Landais, A., Masson-Delmotte, V., Genthon, C., Kerstel, E., Kassi, S., ... Cermak, P. (2016). Continuous measurements of isotopic composition of water vapour on the East Antarctic Plateau. *Atmospheric Chemistry and Physics*, *16*, 8521–8538.

Casado, M., Landais, A., Picard, G., Münch, T., Laepple, T., Stenni, B., ... others (2018). Archival processes of the water stable isotope signal in East Antarctic ice cores. *The Cryosphere*, *12*(5), 1745–1766.

Craig, H. (1961). Standard for reporting concentrations of deuterium and oxygen-18 in natural waters. *Science*, *133*(3467), 1833–1834.

Dar, S. S., Ghosh, P., Swaraj, A., & Kumar, A. (2020). Craig–Gordon model validation using stable isotope ratios in water vapor over the Southern Ocean. *Atmospheric Chemistry and Physics*, *20*(19), 11435–11449.

Fujita, K., & Abe, O. (2006). Stable isotopes in daily precipitation at Dome Fuji, East Antarctica. *Geophysical Research Letters*, *33*(18).

Gat, J. R., Mook, W. G., & Meijer, H. (2001). Environmental isotopes in the hydrological cycle: Principles and Applications. *Technical Documents in Hydrology*, *2*(39).

Gat, J. R., Shemesh, A., Tziperman, E., Hecht, A., Georgopoulos, D., & Basturk, O.

(1996). The stable isotope composition of waters of the eastern Mediterranean Sea. *Journal of Geophysical Research: Oceans*, *101*(C3), 6441–6451.

Horita, J., Rozanski, K., & Cohen, S. (2008). Isotope effects in the evaporation of water: a status report of the Craig–Gordon model. *Isotopes in Environmental and Health Studies*, *44*(1), 23–49.

Hughes, A. G., Wahl, S., Jones, T. R., Zuhr, A., Hörhold, M., White, J. W. C., & Steen-Larsen, H. C. (2021). The role of sublimation as a driver of climate signals in the water isotope content of surface snow: laboratory and field experimental results. *The Cryosphere*, *15*(10), 4949–4974.

Kumar, B., & Nachiappan, R. P. (1999). On the sensitivity of Craig and Gordon Model for the estimation of the isotopic composition of lake evaporates. *Water Resources Research*, *35*(5), 1689–1691.

Landais, A., Ekaykin, A., Barkan, E., Winkler, R., & Luz, B. (2012). Seasonal variations of ^{17} O-excess and d-excess in snow precipitation at Vostok station, East Antarctica. *Journal of Glaciology*, *58*(210), 725–733.

LeGrande, A. N., & Schmidt, G. A. (2006). Global gridded data set of the oxygen isotopic composition in seawater. *Geophysical Research Letters*, *33*(12), L12604.

Majoube, M. (1970). Fractionation factor of 18 O between water vapour and ice. *Nature*, *226*(5252), 1242–1242.

Majoube, M. (1971). Fractionnement en oxygène 18 et en deutérium entre l'eau et sa vapeur. *J. Chim. Phys.*, *68*, 1423–1436.

Masson-Delmotte, V., Hou, S., Ekaykin, A., Jouzel, J., Aristarain, A., Bernardo, R., ... others (2008). A review of antarctic surface snow isotopic composition: Observations,

atmospheric circulation, and isotopic modeling. *Journal of climate*, *21*(13), 3359–3387.

Merlivat, L. (1978). Molecular diffusivities of $H_2{}^{16}O$, $HD^{16}O$, and $H_2{}^{18}O$ in gases. *J. Chem. Phys.*, *69*, 2864–2871.

Merlivat, L., & Nief, G. (1967). Fractionnement isotopique lors des changements d'état solide-vapeur et liquide-vapeur de l'eau à des températures inférieures à 0°C. *Tellus*, *19*(1), 122–127.

Sinclair, K. E., Marshall, S. J., & Moran, T. A. (2011). A Lagrangian approach to modelling stable isotopes in precipitation over mountainous terrain. *Hydrological Processes*, *25*(16), 2481–2491.

Stenni, B., Scarchilli, C., Masson-Delmotte, V., Schlosser, E., Ciardini, V., Dreossi, G., ... others (2016). Three-year monitoring of stable isotopes of precipitation at Concordia Station, East Antarctica. *The Cryosphere*, *10*(5), 2415–2428.

Table S1. Important simulation constants and parameters.

Quantity	Symbol	Value	Unit
Molar mass for $H_2{}^{16}O$	$M_{H_2{}^{16}O}$	0.018	kg mol^{-1}
Molar mass for $H_2{}^{18}O$	$M_{H_2{}^{18}O}$	0.020	kg mol^{-1}
Molar mass for $HD^{16}O$	$M_{HD^{16}O}$	0.019	kg mol^{-1}
Isotopic ratio for VSMOW	$R_{H_2{}^{18}O}$	2.0052×10^{-3}	–
Isotopic ratio for VSMOW	$R_{HD^{16}O}$	1.5595×10^{-4}	–
Ratio of molecular diffusivities	$D_{H_2{}^{18}O}/D_{H_2{}^{16}O}$	0.9727[a]	–
Ratio of molecular diffusivities	$D_{HD^{16}O}/D_{H_2{}^{16}O}$	0.9757[a]	–
Latent heat of evaporation	L_e	2.5×10^6	J kg^{-1}
Number of snow layers	n_{max}	100	–
Snow layer thickness	SLT	0.01[b]	m
Snow density	ρ_s	350	kg m^{-3}
Air parcel volume	V	$1 \times 1 \times 1$	m^3

[a] Merlivat (1978)
[b] Refers to the baseline simulation; other values of 0.001 m and 0.1 m are used in sensitivity tests

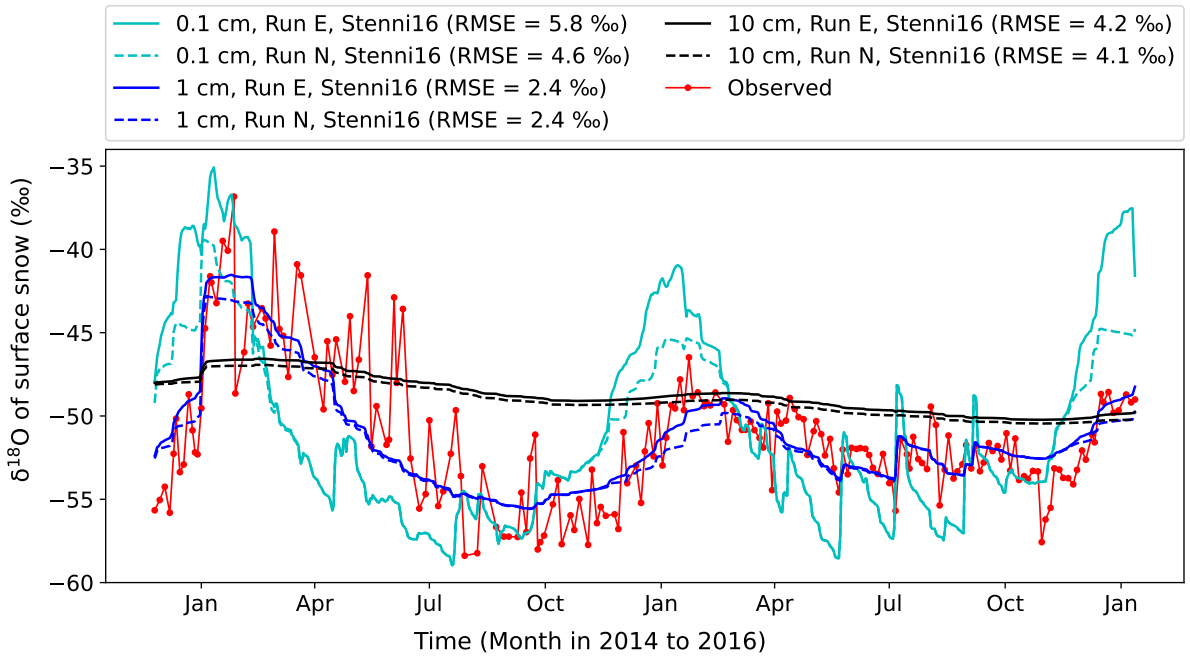

Figure S1. Sensitivity of the modelled δ^{18}O of surface snow at Dome C with respect to snow layer thickness (0.1 cm, 1 cm, or 10 cm) in Run E (solid lines) and Run N (dashed lines) from November 2013 to January 2016. Daily averages are compared with observed samples taken approximately every four days as described in Casado et al. (2018); respective root-mean-square errors are shown in the legend. For this figure, the snowfall $\delta-$temperature relationship of Stenni et al. (2016) is used.

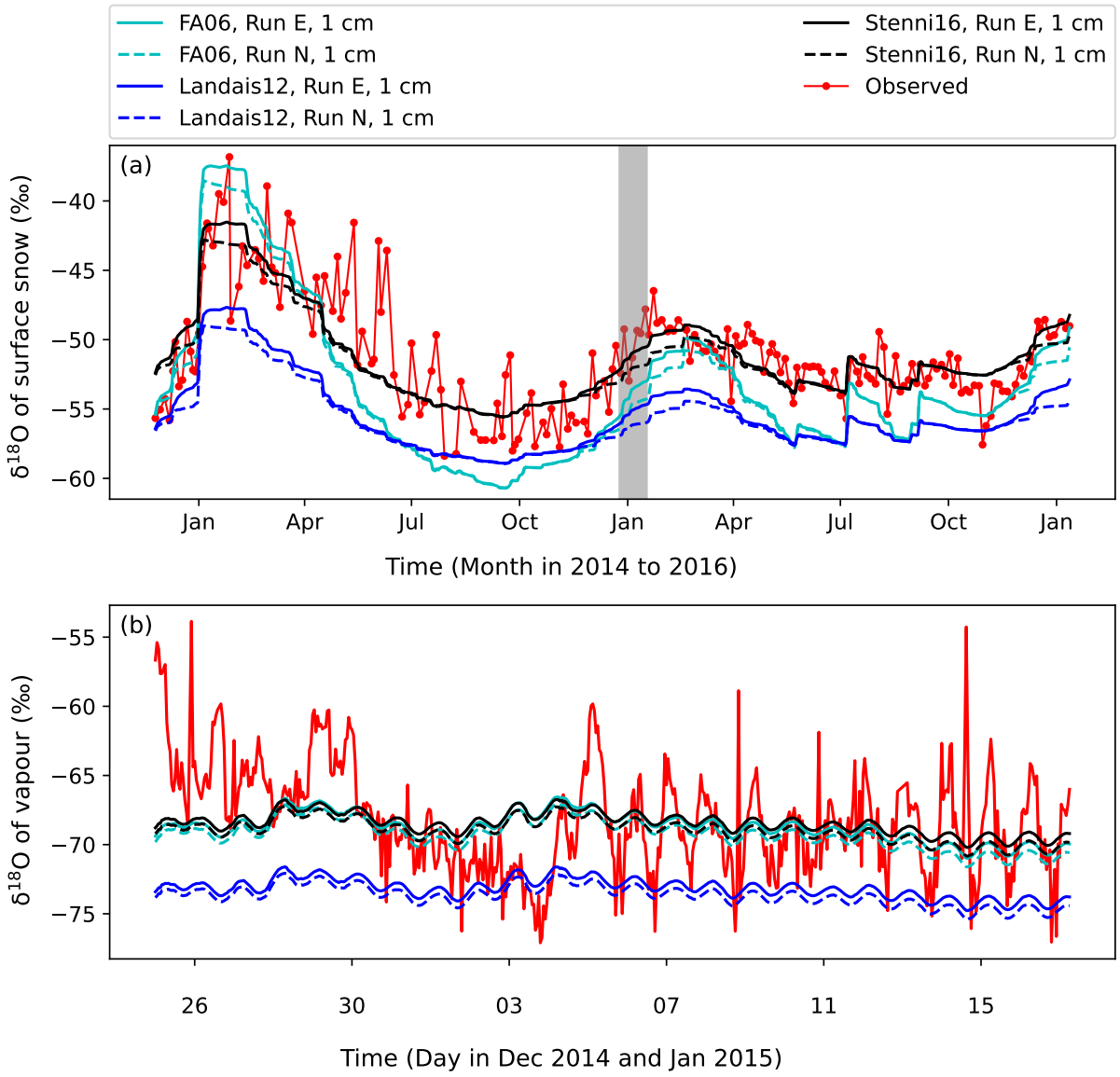

Figure S2. Sensitivity of the modelled δ^{18}O of (a) surface snow and (b) atmospheric water vapour at Dome C with respect to the assumed $\delta-$temperature relationship for snowfall in Run E (solid lines) and Run N (dashed lines) of *Model Sublimation*. In all cases, a snow layer thickness of 1 cm is used. Panel (a) compares hourly averages with observed samples taken approximately every four days as described in Casado et al. (2018). Panel (b) shows hourly values for vapour in the grey-shaded period and the measurements represent running mean values as described in Casado et al. (2016).

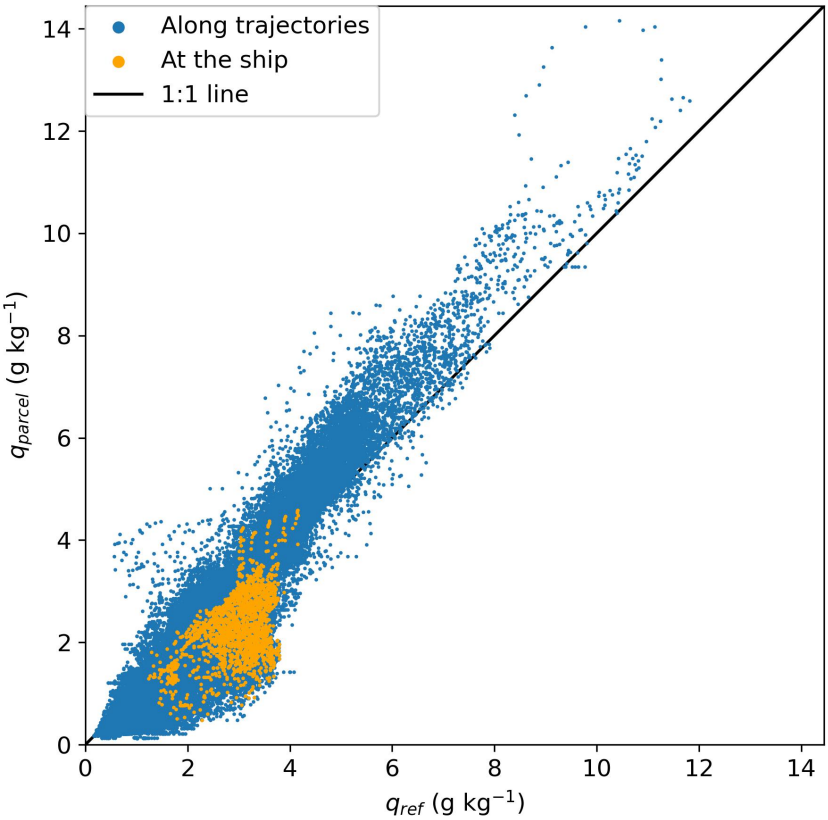

Figure S3. Comparison of the specific humidity between *Model Air Parcel* (q_{parcel}) and the trajectory data set (q_{ref}), which is based on operational analyses of the European Centre for Medium-Range Weather Forcasts.

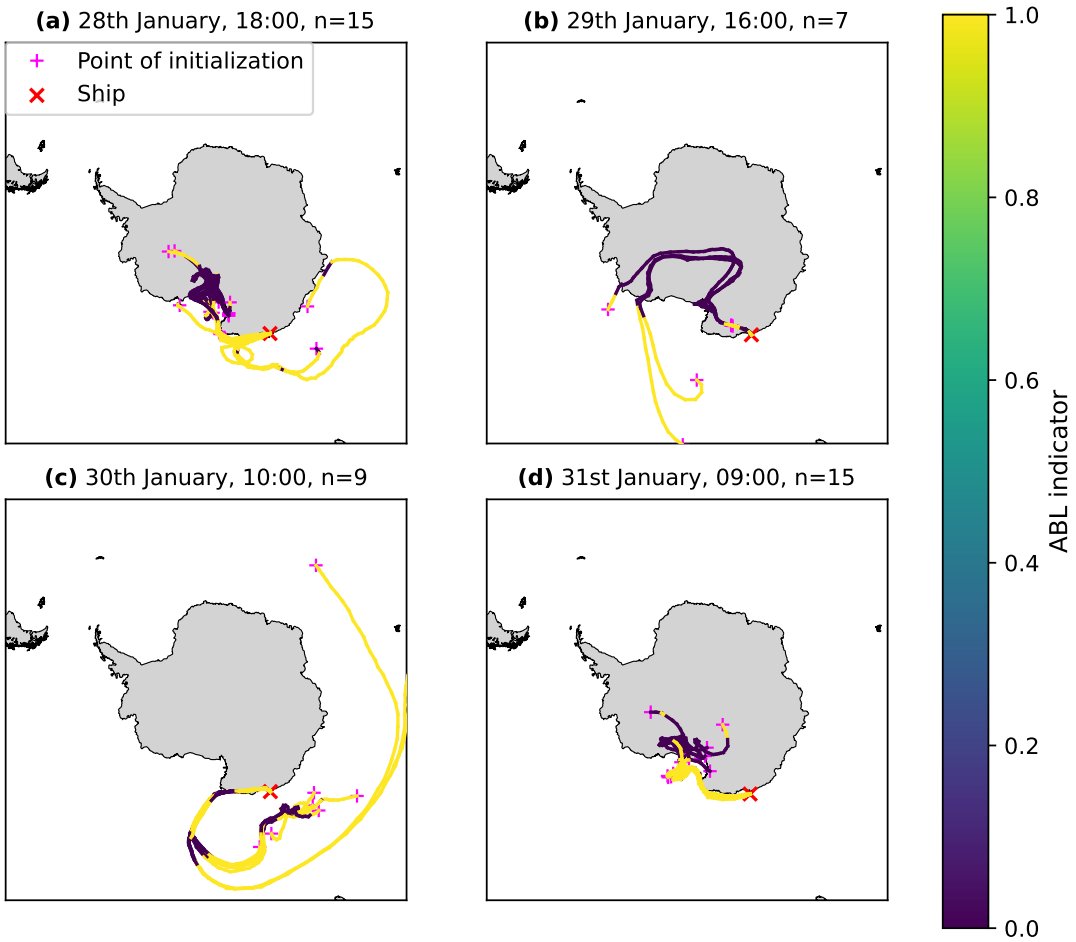

Figure S4. Atmospheric boundary layer (ABL) indicator along air parcel trajectories in the baseline simulation of Run E for four different times of arrival at the ship (same times as in Figure 5 of the main article). The indicator has a value of 1 if the air parcel is in the ABL and a value of 0 otherwise. The number of trajectories is denoted by n. Trajectories arriving at the ship at a lower height are plotted on top of other trajectories.